Low and High Pressure Headaches

Jennifer W McVige MD
Dent Neurologic Institute
American Society for Neuroimaging
2021

THE AMERICAN SOCIETY OF NEUROIMAGING

DENT NEUROLOGIC INSTITUTE

Potential Conflicts of Interest

Research

Allergan/ AbbVie
Amgen/ Novartis
Avanir
Biohaven
Eli Lilly and Company
Lundbeck
Teva

Speaker

Allergan/AbbVie
Amgen
Avanir
Biohaven
Eli Lilly
Lundbeck
Teva

Pressure Related Headaches

- Underdiagnosed and often misdiagnosed
- Many have normal imaging
- Many have normal opening lumbar pressure
- Many have opthalmologic signs that are missed
- Low and High pressure headaches can sometimes have the same symptoms

Pressure Related Headaches

TABLE 6-1 **Overlap of Clinical Features of High and Low Cerebrospinal Fluid Pressure Disorders and Primary Headache Disorders**

Feature	Pseudotumor Cerebri Syndrome	Intracranial Hypotension	Primary Headache Disorder
Location of pain	Often frontal or retro-orbital but varies	Often posterior but varies	Varies
Timing	Worse in the morning or no fluctuation	Worse as the day progresses	Patterns vary by headache type; migraine is often present upon awakening
Nocturnal awakening	Yes	Yes	Yes; frequent in cluster headache, infrequent in migraine, defining of hypnic headache
Worse with Valsalva maneuver, exercise, bending over	Yes	Yes	Yes; migraine, primary exertional headaches, secondary causes (eg, reversible cerebral vasoconstriction syndrome, aneurysm, Chiari malformation)
Effect of caffeine	None or worsens	Improvement	Either; caffeine may provoke migraine or relieve it
Orthostatic/positional component	Sometimes worse lying flat	Usually better lying flat	Varies; patients with migraine often prefer to lie down, which may be related to avoiding movement
Effect of high altitude	Usually worsens	Usually improves	Either; migraine is a risk factor for headache at high altitude[1]
Effect of Trendelenburg position	None (may theoretically worsen)	Often improves	None
Pulsatile tinnitus	Common	Rare (but may have nonpulsatile tinnitus)	Not associated
Transient obscurations of vision	Common	No	No; transient visual loss in migraine lasts longer than 1 to 2 minutes and is not postural
Joint hypermobility	Not associated	Common	Not associated
Neck or back pain	Common	Common	Common
Radicular pain	Common	Rare	No
Papilledema	Usually present	No	No
Spontaneous venous pulsations	Absent	Usually present	Usually present
Associated with cerebral venous sinus thrombosis	Yes	Yes	No
Sex	Marked female preponderance after puberty	More common in females	Male or female; depends on primary headache diagnosis
Body habitus	Usually obese	Often slim or normal	No association

Freidman, D Headaches due to low and high intracranial pressure Continuum 2018;24(4) Headache:1066-1091

Low Pressure Headaches Diagnosis

Diagnostic Criteria for Spontaneous Cerebrospinal Fluid Leak and Intracranial Hypotension[a]

A **Demonstration of a spinal CSF leak (ie, presence of extrathecal CSF)**
Or, if criterion A not met,

B **Cranial MRI changes of intracranial hypotension (ie, presence of subdural fluid collections, enhancement of the pachymeninges, or sagging of the brain) and the presence of at least one of the following:**

1. Low opening pressure (≤60 mm H_2O)
2. Spinal meningeal diverticulum
3. Improvement of symptoms after epidural blood patching

Or, if criteria A and B not met:

C **The presence of all of the following or at least two of the following if typical orthostatic headaches are present:**

1. Low opening pressure (≤60 mm H_2O)
2. Spinal meningeal symptoms
3. Improvement of symptoms after epidural blood patching

Note: Patients with onset of symptoms after dural puncture or other penetrating spinal trauma are excluded.

Prevalence 1 per 50,000
Incidence 5 per 100,000

- Women
- 40-50 yrs old

Freidman, D Headaches due to low and high intracranial pressure Continuum 2018;24(4) Headache:1066-1091

Low Pressure Headaches Causes

Table 1. Etiology of CSF Leak, CSF Volume Depletion, or CSF Hypovolemia

1. True hypovolemic state (reduced total body water)
2. Traumatic CSF leaks
   a. Definite trauma (MVAs, sports injuries, etc)
   b. Thecal holes and rents from LPs and epidural catheterizations
   c. Spinal and cranial surgeries including skull base and some sinus surgeries
   d. Proximal brachial plexus avulsion injuries, nerve root avulsions
3. CSF shunt overdrainage
4. Spontaneous CSF leaks
   a. Undetermined cause
   b. Preexisting weakness of the dural sac, surgical anatomical observations
      i. Meningeal diverticula
      ii. Disorders of connective tissue matrix
         1. Marfan syndrome, Marfanoid features
         2. Joint hypermobility
         3. Retinal detachment at young age
         4. Abnormalities of elastin and fibrillin in cultured dermal fibroblasts
   c. Trivial trauma in the setting of preexisting dural weakness
   d. Spondylotic spurs, herniated discs

Mokri, B Spontaneous Low Pressure, Low CSF Volume Headaches: Spontaneous CSF Leaks Headache 2013;53:1034-53

Low Pressure Headaches

Mokri, B Spontaneous Low Pressure, Low CSF Volume Headaches: Spontaneous CSF Leaks Headache 2013;53:1034-53

Joint hypermobility (left upper), skin hyperelasticity (left lower), and multiple meningeal diverticula (right) in a patient with spontaneous cerebrospinal fluid (CSF) leak, suggestive of an underlying disorder of connective tissue matrix (with permission of Mayo Foundation).

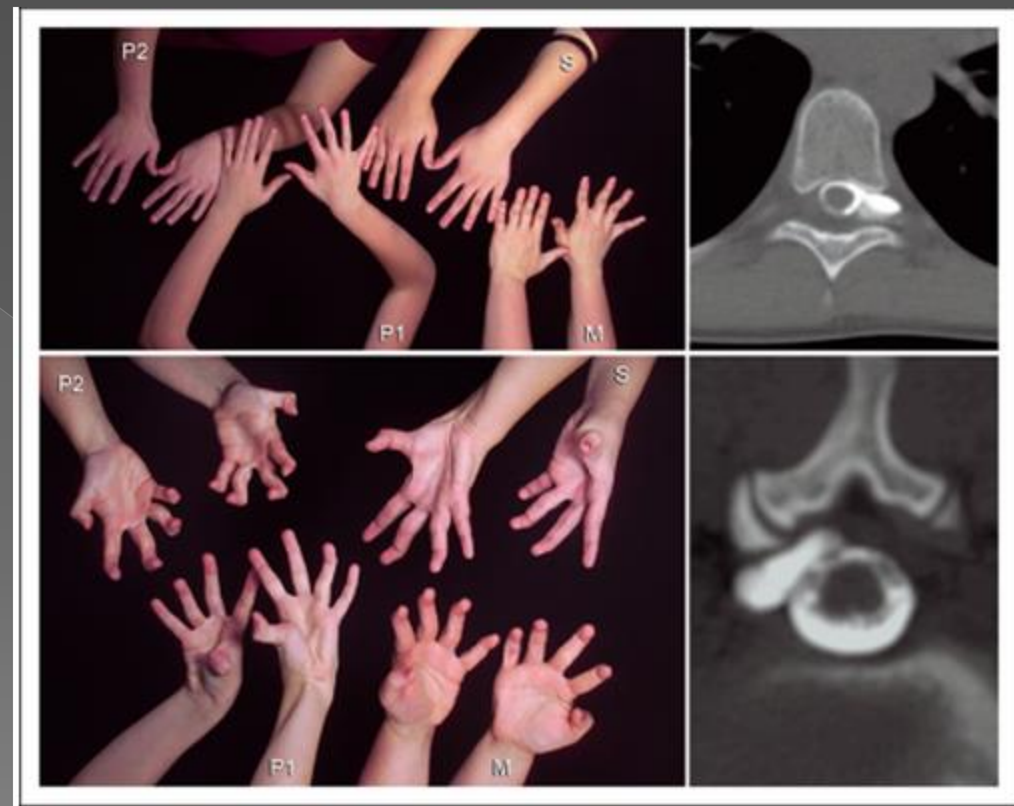

Familial spontaneous cerebrospinal fluid (CSF) leak and joint hypermobility. Note fingers at rest (left upper) and at contraction (left lower). Joint hypermobility and interphalangeal (IP) joint subluxations are seen in all. P1 and P2: the two sisters with CSF leak. S: the sister who had not developed CSF leak. M: the mother. CT myelogram in the two sisters with CSF leak (right upper and lower). Both show leaking meningeal diverticula (from Mokri B, Ref 20, with permission of *Headache*).

Spontaneous Intracranial Hypotension

CSF leak→
loss CSF volume→

compensation with subdural collection →
increased intracranial blood →

pachymeningeal enhancement →
enlarged pituitary →
enlarged venous sinus

Mokri, B Spontaneous Low Pressure, Low CSF Volume Headaches: Spontaneous CSF Leaks Headache 2013;53:1034-53

MRI Brain Abnormalities CSF Leak

Table 3. Head MRI Abnormalities in CSF Leaks

1. Diffuse pachymeningeal enhancement:[†] uninterrupted, non-nodular, can be thick or thin, no leptomeningeal abnormality
2. Descent ("sagging" or "sinking") of the brain
   a. Descent of cerebellar tonsils at or below the foramen magnum (may mimic type I Chiari)86
   b. Descent of the brainstem and mesencephalon, occasionally without descent of cerebellar tonsils to or below foramen magnum
   c. Increase in anteroposterior diameter brainstem resulting from distortion of the brainstem
   d. Descent of iter[‡] below the incisural line[§]9
   e. Obliteration of prepontine or perichiasmatic cisterns
   f. Crowding of the posterior fossa
   g. Flattening of the optic chiasm
   h. Flattening of the anterior pons
3. Subdural fluid collections, typically hygromas, infrequently hematomas
4. Enlargement of the pituitary (may mimic pituitary tumor or hyperplasia)87
5. Engorged cerebral venous sinuses
6. Decrease in size of the ventricles ("ventricular collapse")

Mokri, B Spontaneous Low Pressure, Low CSF Volume Headaches: Spontaneous CSF Leaks Headache 2013;53:1034-53

MRI Spine Abnormalities CSF Leak

Table 4. Spine MRI Abnormalities in Spontaneous CSF Leaks

1. Extra-arachnoid fluid collections (often extending along several spinal levels)[88-90]
2. Extradural extravasation of fluid (extending to paraspinal soft tissues)
    a. May identify the level of the leak (ie, cervical, thoracic or lumbar), not uncommon
    b. May identify the actual site of the leak, uncommon[91]
3. Meningeal diverticula,[a] single or multiple, various sizes, any level of spine
4. Spinal dural enhancement[92]
5. Engorgement of spinal epidural venous plexus

Mokri, B Spontaneous Low Pressure, Low CSF Volume Headaches: Spontaneous CSF Leaks Headache 2013;53:1034-53

CSF Leak Imaging

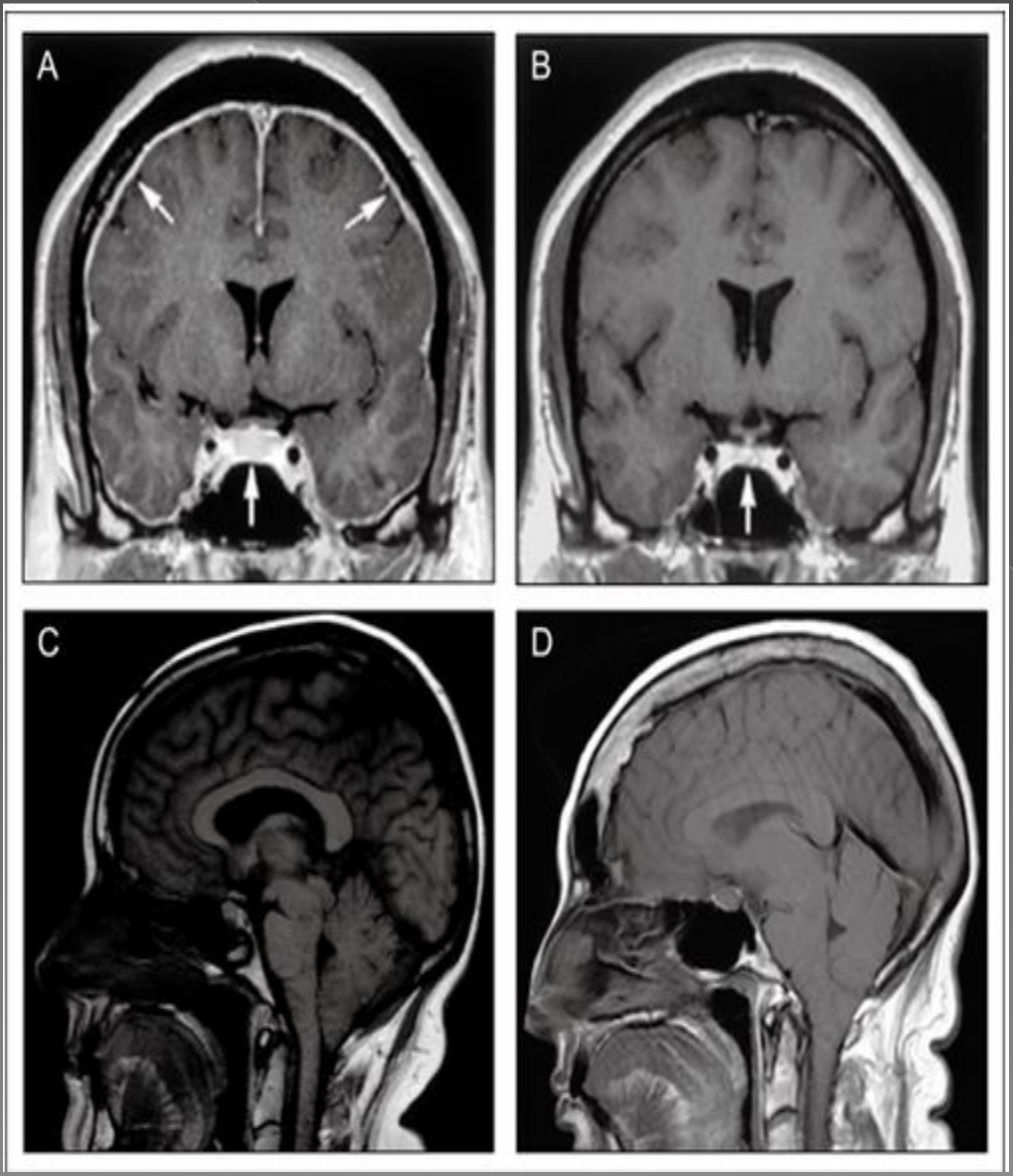

Head magnetic resonance imaging (MRI) in cerebrospinal fluid (CSF) leak – CSF hypovolemia. Upper panels show T1-weighted gadolinium-enhanced coronal images at the level of sella-pituitary (A) during active leak; (B) after surgical treatment of a leaking meningeal diverticulum. Note diffuse pachymeningeal enhancement (upper arrows), enlarged pituitary, flattening of the optic chiasm, smaller perichiasmatic cistern, and lateral ventricles in (A); all resolved after cessation of the leak in (B). (C) Shows descent of the cerebellar tonsils below the foramen magnum. (D) Shows descent of the cerebellar tonsils and brainstem, increase in AP diameter and deformity of brainstem, crowded posterior fossa, obliteration of prepontine cistern and flattening of anterior pons all related to the sinking of the brain (A and B from Mokri B, Ref 52, with permission of Mayo Foundation).

Mokri, B Spontaneous Low Pressure, Low CSF Volume Headaches: Spontaneous CSF Leaks Headache 2013;53:1034-53

CSF Leak Imaging

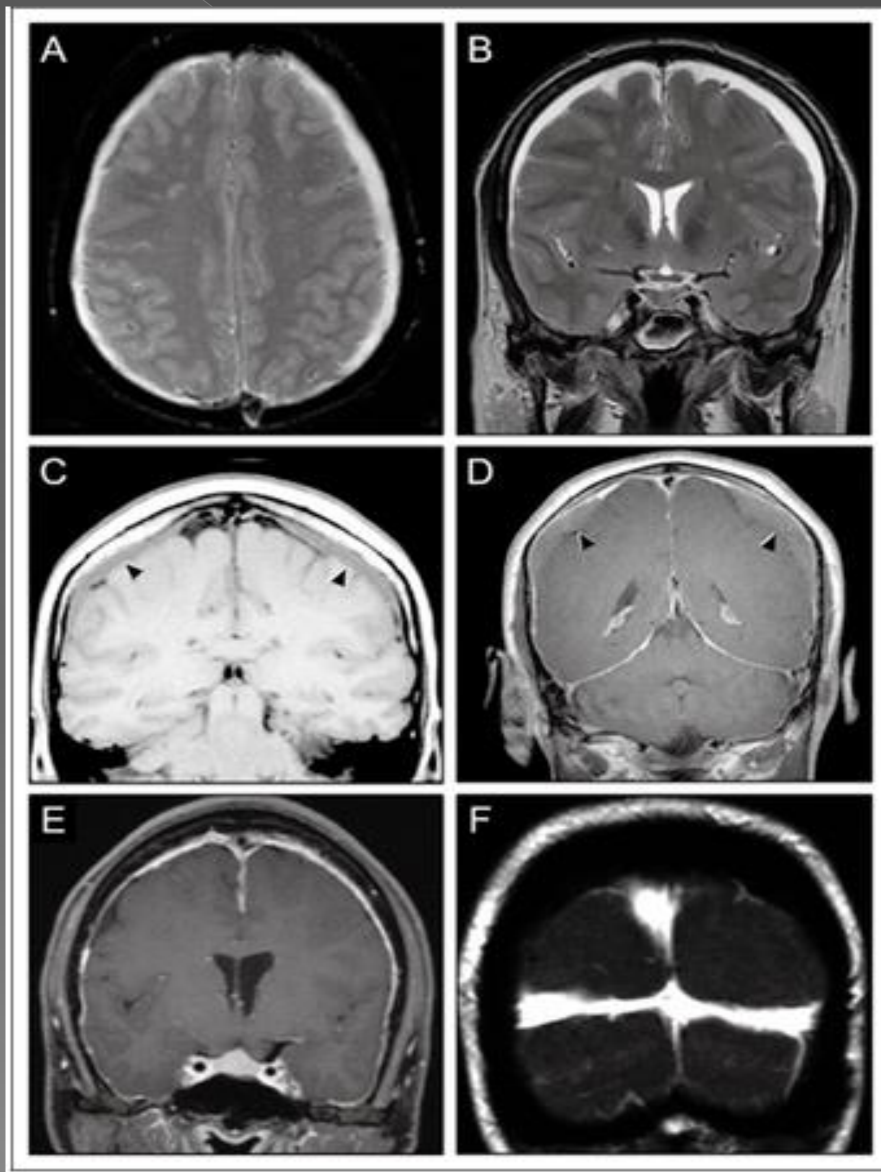

Figure 7 Open in figure viewer PowerPoint

Head magnetic resonance imaging (MRI) in cerebrospinal fluid (CSF) leak - CSF hypovolemia. (A) and (B) Subdural fluid collections. (C) Bilateral subdural collections with signal characteristics different from the CSF (arrows), likely related to increased protein concentration or blood-tinged fluid. (D) Bilateral subdural hematomas with mass effect on underlying brain (arrows). (E) Enlarged pituitary and obliteration of the perichiasmatic cistern. (F) Engorged cerebral venous sinuses.

Mokri, B Spontaneous Low Pressure, Low CSF Volume Headaches: Spontaneous CSF Leaks Headache 2013;53:1034-53

Low CSF Pressure Headaches

Importance of various imaging modalities

Modality	Advantages	Disadvantages
HRCT	Bony defect characterization	Radiation, differentiation from mucosal pathology is difficult
CT cisternography	Accuracy in bony defect detection, characterization of defect, less time	Radiation, invasive, poor patient acceptance, intermittent leak may be missed
MR cisternography	No radiation, noninvasive, good patient acceptance	Lack of bony detail, false negatives
Radionuclide cisternography	Intermittent leaks can be detected	Radiation, invasive, poor patient acceptance, lengthy procedure

HRCT: High resolution computed tomography, MR: Magnetic resonance

Unlike CT cisternography, MR cisternography does not require an active CSF leak to demonstrate the site of leak. Inactive leaks are often under-diagnosed on CT cisternography. Both active and inactive leaks can be diagnosed on MR cisternography. Another important and robust advantage of MR cisternography is the detection of spontaneous leaks. Many of the spontaneous leaks might be associated with cephaloceles and encephaloceles. Cephaloceles are easier to be missed on CT but can be confidently diagnosed on MRI. The major disadvantage of MR cisternography is the lack of bony detail. The gradient-echo images greatly improved the detail of the osseous anatomy in the skull base, but still the osseous anatomy is better appreciated with CT imaging rather than with MRI. A diagnostic algorithm [Figure 12] Lloyd *et al*.[1] has been postulated to carry out sequential imaging for accurate diagnosis.

Vemuri, N et al Imaging review of CSF leaks
Indian J Radiol Imaging. 2017 Oct-Dec; 27(4): 441–446.

Low CSF Pressure Headaches

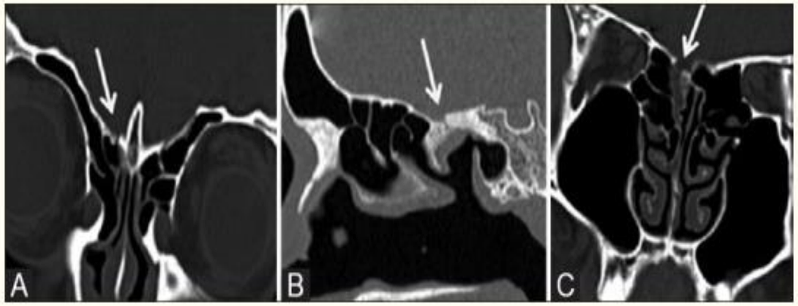

Figure 2(A-C)

CT scan of Paranasal sinuses showing (A) Osseous defects at Fovea Ethmoidalis (B and C) soft tissue density adjacent to osseous defect

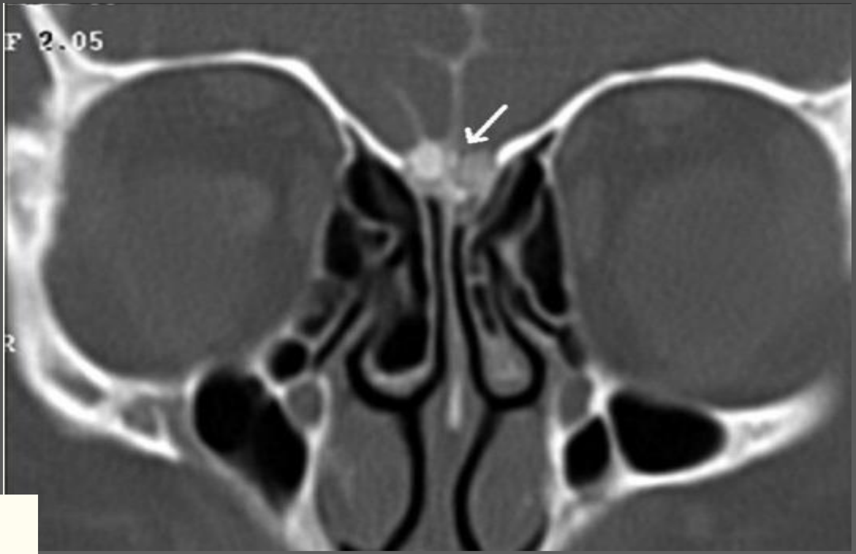

Figure 3

CT Cisternography showing active leak thru left cribriform plate

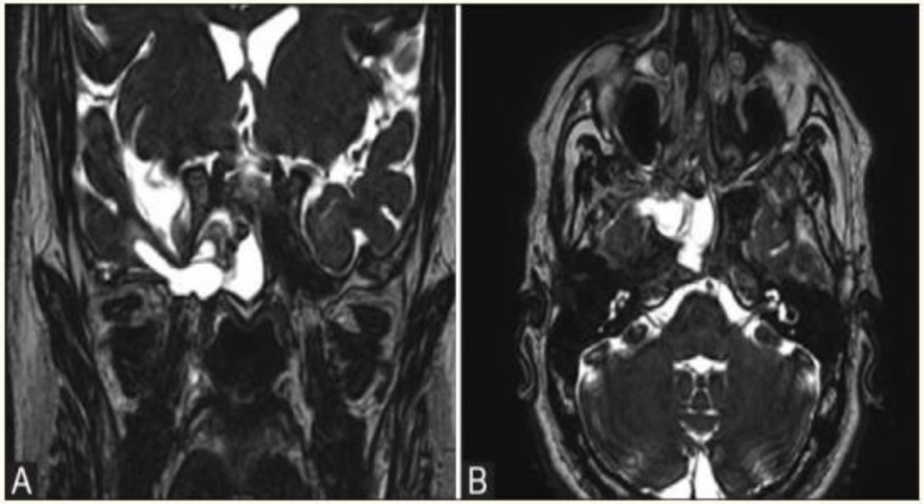

Figure 6(A and B)

52 year old man with spontaneous CSF rhinorrhoea, coronal and axial T2 DRIVE MR images demonstrating CSF fistula into right sphenoid sinus thru osseous defect of inferolateral wall of sphenoid sinus

Vemuri, N et al Imaging review of CSF leaks
Indian J Radiol Imaging. 2017 Oct-Dec; 27(4): 441–446.

Myelographic Techniques for the Detection of Spinal CSF Leaks in Spontaneous Intracranial Hypotension

Peter G. Kranz[1], Patrick H. Luetmer[2], Felix E. Diehn[2], Timothy J. Amrhein[1] ... Show all

American Journal of Roentgenology. 2016;206: 8-19. 10.2214/AJR.15.14884

View larger version (360K)

Fig. 1A —40-year-old woman with CSF leak caused by meningeal diverticulum.

A, Axial CT myelography (CTM) image shows focal diverticulum (*arrow*) located anterior to nerve root sleeve.

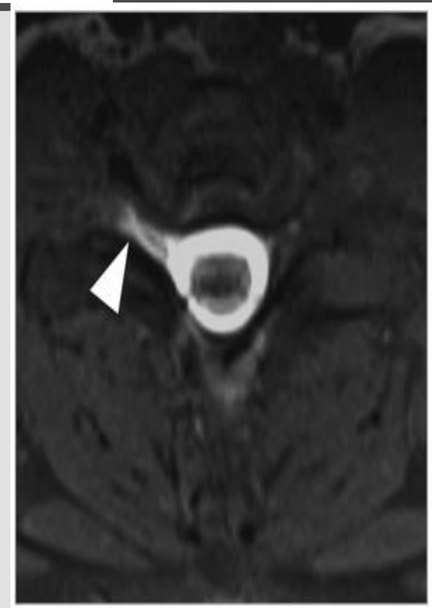

View larger version (170K)

Fig. 9B —27-year-old woman who underwent MR myelography with intrathecal gadolinium.

B, Axial T1-weighted image with fat suppression after intrathecal gadolinium administration through same level much more clearly shows contrast material leaking along right C8 nerve root (*arrowhead*).

View larger version (365K)

Fig. 1C —40-year-old woman with CSF leak caused by meningeal diverticulum.

C, Image from conventional myelogram performed with patient in left lateral decubitus position shows dependent layering of contrast material in diverticulum (*arrow*). Contrast material is seen leaking into epidural space (*arrowhead*) from this level.

Some studies have shown MRM maybe 20% more sensitive but there are risks to using the intrathecal gadolinium off label due toxicity with high doses. It is better with slow leaks.

Compared with CTM, MRI has the advantage of being noninvasive and does not involve ionizing radiation. However, MRI typically does not localize the exact leak site, generally suffers from more artifacts, has lower spatial resolution than CTM, and requires very homogeneous suppression of fat signal to detect more subtle leaks.

Low CSF Pressure Headaches Digital Subtraction Myelography

Spontaneous Intracranial Hypotension: A Systematic Imaging Approach for CSF Leak Localization and Management Based on MRI and Digital Subtraction Myelography

R.I. Farb, P.J. Nicholson, P.W. Peng, E.M. Massicotte, C. Lay, T. Krings and K.G. terBrugge

American Journal of Neuroradiology April 2019, 40 (4) 745-753; DOI: https://doi.org/10.3174/ajnr.A6016

ABSTRACT

BACKGROUND AND PURPOSE: Localization of the culprit CSF leak in patients with spontaneous intracranial hypotension can be difficult and is inconsistently achieved. We present a high yield systematic imaging strategy using brain and spine MRI combined with digital subtraction myelography for CSF leak localization.

MATERIALS AND METHODS: During a 2-year period, patients with spontaneous intracranial hypotension at our institution underwent MR imaging to determine the presence or absence of a spinal longitudinal extradural collection. Digital subtraction myelography was then performed in patients positive for spinal longitudinal extradural CSF collection primarily in the prone position and in patients negative for spinal longitudinal extradural CSF collection in the lateral decubitus positions.

RESULTS: Thirty-one consecutive patients with spontaneous intracranial hypotension were included. The site of CSF leakage was definitively located in 27 (87%). Of these, 21 were positive for spinal longitudinal extradural CSF collection and categorized as having a ventral (type 1, fifteen [48%]) or lateral dural tear (type 2; four [13%]). Ten patients were negative for spinal longitudinal extradural CSF collection and were categorized as having a CSF-venous fistula (type 3, seven [23%]) or distal nerve root sleeve leak (type 4, one [3%]). The locations of leakage of 2 patients positive for spinal longitudinal extradural CSF collection remain undefined due to resolution of spontaneous intracranial hypotension before repeat digital subtraction myelography. In 2 (7%) patients negative for spinal longitudinal extradural CSF collection, the site of leakage could not be localized. Nine of 21 (43%) patients positive for spinal longitudinal extradural CSF collection were treated successfully with an epidural blood patch, and 12 required an operation. Of the 10 patients negative for spinal longitudinal extradural CSF collection (8 localized), none were effectively treated with an epidural blood patch, and all have undergone ($n = 7$) or are awaiting ($n = 1$) an operation.

CONCLUSIONS: Patients positive for spinal longitudinal extradural CSF collection are best positioned prone for digital subtraction myelography and may warrant additional attempts at a directed epidural blood patch. Patients negative for spinal longitudinal extradural CSF collection are best evaluated in the decubitus positions to reveal a CSF-venous fistula, common in this population. Patients with CSF-venous fistula may forgo further epidural blood patch treatment and go on to surgical repair.

Low CSF Pressure Headaches Digital Subtraction Myelography

Spontaneous Intracranial Hypotension: A Systematic Imaging Approach for CSF Leak Localization and Management Based on MRI and Digital Subtraction Myelography

R.I. Farb, P.J. Nicholson, P.W. Peng, E.M. Massicotte, C. Lay, T. Krings and K.G. terBrugge

American Journal of Neuroradiology April 2019, 40 (4) 745-753; DOI: https://doi.org/10.3174/ajnr.A6016

FIG 1. Spinal longitudinal extradural collections. *A*, Sagittal T2 FSE. *B*, Reformatted axial T2 SPACE images show SLECs (*arrows*) and displaced dura outlined by the CSF. *C* and *D*, Images similar to *A* and *B* of the same patient show similar findings in the lower thoracic region.

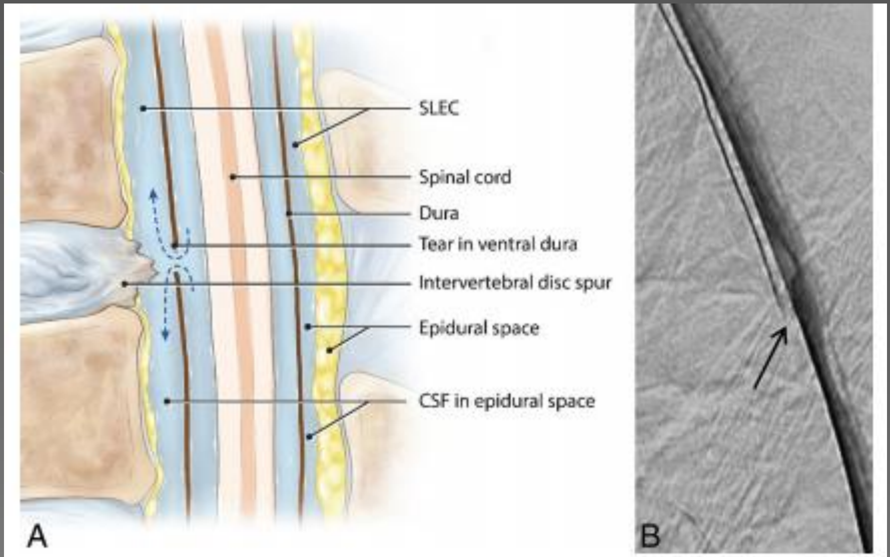

FIG 2. Type 1 CSF leak (SLEC-P). *A*, Schematic drawing shows the relationship of the intervertebral disc spur and a ventral dural tear. *B*, "Shoot though" lateral subtracted image of the thoracic spine DSM with the patient positioned prone on the table. The patient's head is toward the top of the image and feet at the bottom. The contrast material can be seen escaping from the ventral aspect of the thecal sac at the T7–8 level (*arrow*).

Low CSF Pressure Headaches
Digital Subtraction Myelography

Spontaneous Intracranial Hypotension: A Systematic Imaging Approach for CSF Leak Localization and Management Based on MRI and Digital Subtraction Myelography

R.I. Farb, P.J. Nicholson, P.W. Peng, E.M. Massicotte, C. Lay, T. Krings and K.G. terBrugge

American Journal of Neuroradiology April 2019, 40 (4) 745-753; DOI: https://doi.org/10.3174/ajnr.A6016

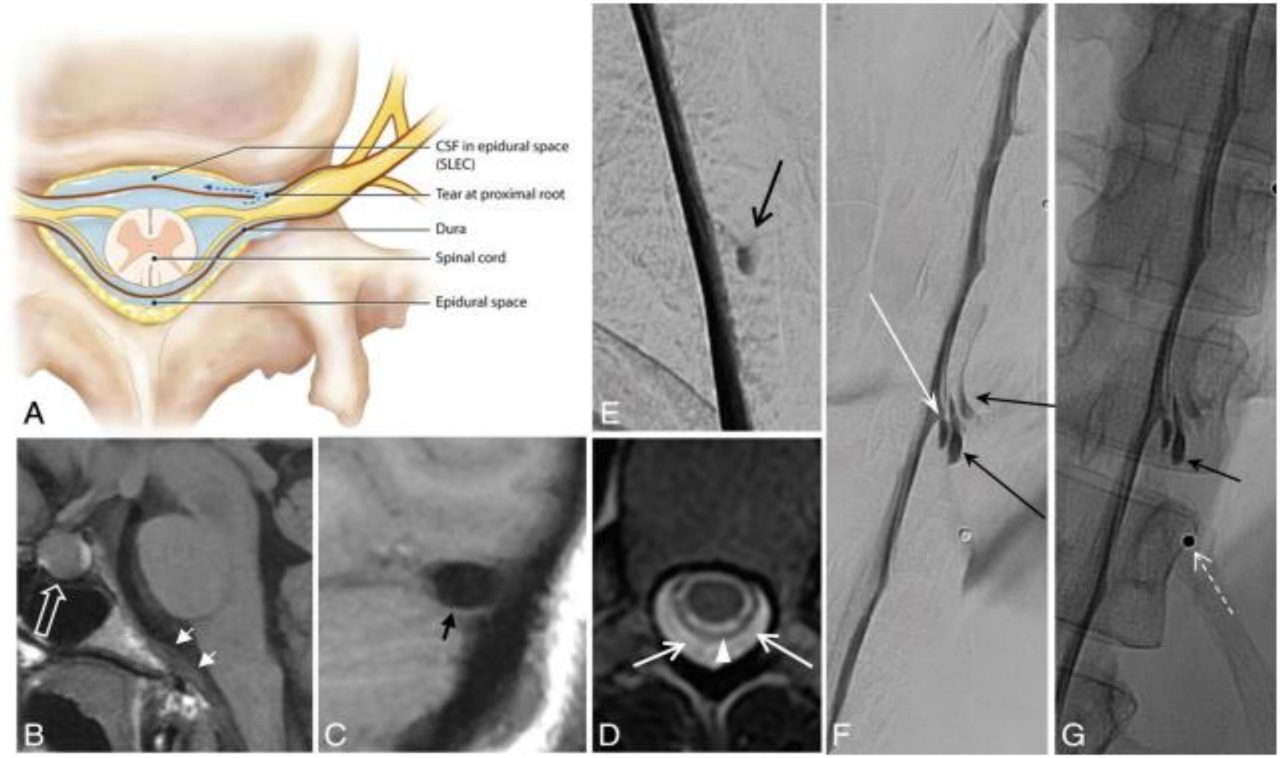

FIG 3. Type 2 CSF leak (SLEC-P). *A*, Schematic depiction of a proximal nerve root sleeve tear bridging the epidural and neural foraminal compartments. *B–G*, From a single patient. *B*, Sagittal T1WI of the brain shows the engorged pituitary gland (*open white arrow*) and dural thickening on the clivus (*short white arrows*). *C*, Sagittal T1WI of the brain shows a "positive venous distension sign" with a convex undersurface of the middle third of the dominant transverse sinus (*short black arrow*). *D*, T2-weighted axial MR image of the thoracic spine shows SLECs (*white arrows*) external to the dura (*white arrowhead*). *E*, Subtracted image from a prone thoracic DSM shows a posterolateral collection of contrast (*black arrow*). *F* and *G*, Subtracted and nonsubtracted images from a repeat right lateral decubitus DSM show contrast leaking into the extradural space (*black arrows*) from a tear along the proximal aspect of the right T11 root sleeve (*long white arrow*). Note the BB (*nipple marker*) placed on the skin for landmarking (*dashed white arrow*).

Intracranial Hypotension: Improved MRI Detection With Diagnostic Intracranial Angles

Lubdha M. Shah[1], Logan A. McLean[1], Marta E. Heilbrun[1], and Karen L. Salzman[1]

American Journal of Roentgenology. 2013;200: 400-407. 10.2214/AJR.12.8611

ABSTRACT Choose

OBJECTIVE. Intracranial hypotension is an uncommon cause of headaches that is often misdiagnosed. The classic MRI features of intracranial hypotension can be variable and subjective. The purpose of this study was to provide objective criteria in the MRI evaluation of intracranial hypotension by quantifying normal values for the pontomesencephalic angle, mamillopontine distance, and lateral ventricular angle.

MATERIALS AND METHODS. A retrospective review of patients with the clinical diagnosis of intracranial hypotension and a control group was performed with measurements of the pontomesencephalic angle, mamillopontine distance, and lateral ventricular angle. Qualitative evaluation of other MRI findings included dural enhancement, venous engorgement, subdural collections, brainstem slumping, and tonsillar herniation.

RESULTS. In 29 patients with intracranial hypotension, the mean pontomesencephalic angle, mamillopontine distance, and lateral ventricular angle were 41.2° (SD, ± 17.4°), 4.4 mm (SD, ± 1.8), and 130.1° (SD, ± 9.8°), respectively. In the control group, the mean pontomesencephalic angle, mamillopontine distance, and lateral ventricular angle were 65° (SD, ± 9.9°), 7.0 mm (SD, ± 1.3), and 132.2° (SD, ± 5.7°), respectively. The differences in the pontomesencephalic angle and mamillopontine distance values for the intracranial hypotension group versus the control group were statistically significant ($p < 0.01$). The difference in the lateral ventricular angle measurements was not statistically significant ($p = 0.37$). Cutoff points of a 5.5-mm mamillopontine distance and 50° pontomesencephalic angle were estimated using receiver operating characteristic curves.

CONCLUSION. In patients with the clinical suspicion of intracranial hypotension, we found that cutoff values of 5.5 mm or less for the mamillopontine distance and 50° or less for the pontomesencephalic angle were sensitive and specific in strengthening the qualitative MRI findings. Therefore, quantitative assessments may provide a more accurate diagnosis.

Intracranial Hypotension: Improved MRI Detection With Diagnostic Intracranial Angles

Lubdha M. Shah[1], Logan A. McLean[1], Marta E. Heilbrun[1], and Karen L. Salzman[1]

American Journal of Roentgenology. 2013;200: 400-407. 10.2214/AJR.12.8611

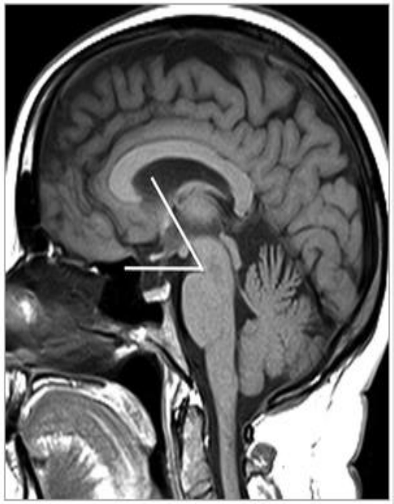

View larger version (216K)

Fig. 1A —Healthy 41-year-old woman (control subject).

A, Pontomesencephalic angle is defined as angle between line drawn along anterior margin of midbrain and anterior superior margin of pons (*lines*). Mean value in patients with intracranial hypotension was 41.2° (SD, ± 17.4°)

Pontomesencephalic Angle

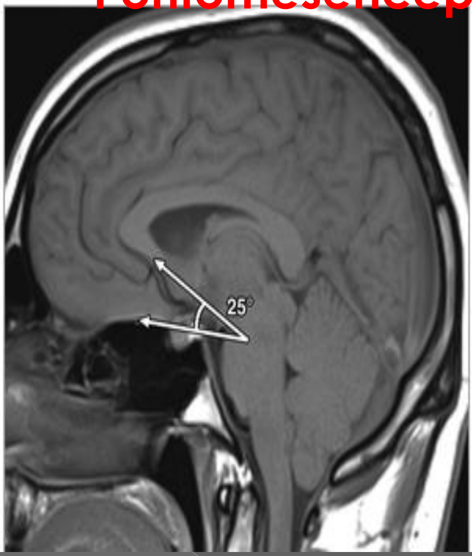

Fig. 2A —Diagnostic intracranial angles in patient with intracranial hypotension.

A, 31-year-old man with 3-month history of positional headaches and neck stiffness. Pontomesencephalic angle is narrowed to 25° (*dashed lines*) as measured on PACS using standard angle-measuring tool. Note also low-lying cerebellar tonsils and brainstem slumping.

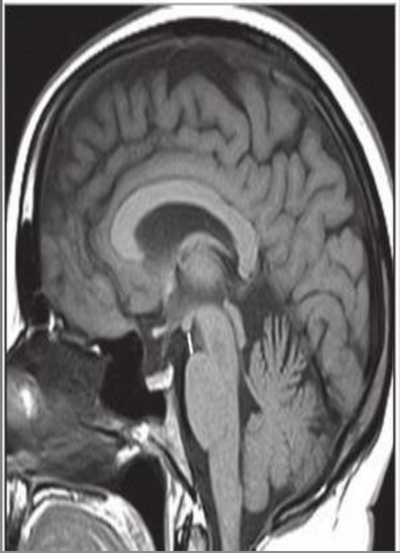

Fig. 1B —Healthy 41-year-old woman (control subject).

B, Mamillopontine distance is defined as distance between inferior aspect of mamillary bodies to superior aspect of pons (*line*). Mean value in patients with intracranial hypotension was 4.4 mm (SD, ± 1.8).

Mamillopontine Distance

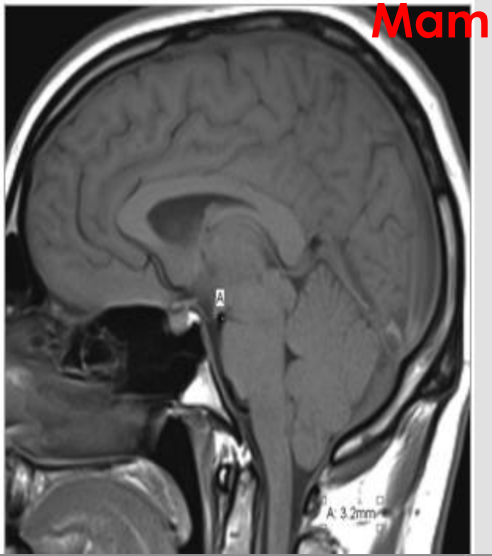

Fig. 2B —Diagnostic intracranial angles in patient with intracranial hypotension.

B, 31-year-old man with 3-month history of positional headaches and neck stiffness. Mamillopontine distance (A) is narrowed to 3.2 mm as measured on PACS using standard ruler tool. Note also brainstem slumping and downward retraction of pituitary infundibulum. There is also mild cerebellar tonsillar displacement.

Treatment

Strategies for Conservative Management of Spontaneous Intracranial Hypotension

- Bedrest (patients can be bedbound because of their symptoms)
- Elevate the foot of the bed (home Trendelenburg position)
- Caffeine, theophylline (often helpful but may produce anxiety and insomnia)
- Abdominal binder
- Analgesics
- Corticosteroids (2- to 4-week gradual prednisone taper starting with 50 mg/d)[24]
- Bilateral greater occipital nerve blocks[25]
- Overhydration
- Time

- Epidural blood patch targeted /nontargeted (10-20 ml autologous blood) – 30% success rate
- Surgery for meningeal tear that will not heal or bony for abnormality

Freidman, D Headaches due to low and high intracranial pressure
Continuum 2018;24(4) Headache:1066-1091

High Pressure Headaches

- Boys and girls are affected equally until puberty, then women > men
- <u>Headaches in 80-90%- </u>frontal pain, throbbing/pressure, posterior, occular and neck pain, global or unilateral, typical sono/photophobia, N/V
- Elevated LP opening pressure

Freidman, D Headaches due to low and high intracranial pressure
Continuum 2018;24(4) Headache:1066-1091

High Pressure Headache Diagnosis

Diagnostic Criteria for the Pseudotumor Cerebri Syndrome[a]

1 Required for Diagnosis of Pseudotumor Cerebri Syndrome[b]

- A Papilledema
- B Normal neurologic examination except for cranial nerve abnormalities
- C Neuroimaging: normal brain parenchyma without evidence of hydrocephalus, mass, or structural lesion and no abnormal meningeal enhancement on MRI, with and without gadolinium, for typical patients (female and obese), and MRI, with and without gadolinium, and magnetic resonance venography for others; if MRI is unavailable or contraindicated, contrast-enhanced CT may be used
- D Normal CSF composition
- E Elevated lumbar puncture opening pressure (≥250 mm CSF in adults and ≥280 mm CSF in children [≥250 mm CSF if the child is not sedated and not obese]) in a properly performed lumbar puncture

2 Diagnosis of Pseudotumor Cerebri Syndrome Without Papilledema

- A In the absence of papilledema, a diagnosis of pseudotumor cerebri syndrome can be made if B–E from above are satisfied and, in addition, the patient has a unilateral or bilateral abducens nerve palsy
- B In the absence of papilledema or sixth nerve palsy, a diagnosis of pseudotumor cerebri syndrome can be suggested but not made if B–E from above are satisfied and, in addition, at least three of the following neuroimaging criteria are satisfied:
  - i Empty sella
  - ii Flattening of the posterior aspect of the globe
  - iii Distention of the perioptic subarachnoid space with or without a tortuous optic nerve
  - iv Transverse venous sinus stenosis

- Benign intracranial hypertension (Pseudotumor cerebri)
- Incidence 0.9 per 100,000
- Incidence in women 3.5 per 100,00
- Incidence in women with obesity 19 per 100,000
- 5% of patients report family history

Freidman, D Headaches due to low and high intracranial pressure Continuum 2018;24(4) Headache:1066-1091

Chen, J., & Wall, M. (2014). Epidemiology and risk factors for idiopathic intracranial hypertension. *International ophthalmology clinics*, *54*(1), 1–11.

High Pressure Headaches Causes

Causes of Pseudotumor Cerebri Syndrome and Commonly Associated Conditions[a] TABLE 6-7

Primary Pseudotumor Cerebri Syndrome

- **Idiopathic intracranial hypertension**

Secondary Pseudotumor Cerebri Syndrome

- **Cerebral venous abnormalities**
  - Cerebral venous sinus thrombosis
  - Jugular vein obstruction
- **Decreased CSF absorption from previous intracranial infection or subarachnoid hemorrhage**
  - Increased right heart pressure
  - Superior vena cava syndrome
- **Associated with systemic venous hypertension**
- **Medications and exposures**
  - Antibiotics (tetracycline family, fluoroquinolones, nalidixic acid)[33]
  - Vitamin A and retinoids (including isotretinoin, all-transretinoic acid, hypervitaminosis A)
  - Hormones
    - Human growth hormone
    - Thyroxine (in children)
    - Leuprorelin acetate
  - Anabolic steroids
  - Withdrawal from chronic corticosteroids
  - Lithium
  - Chlordecone
- **Medical conditions**
  - Endocrine disorders (Addison disease, hypoparathyroidism)
  - Hypercapnia (sleep apnea, pickwickian syndrome)
  - Anemia
  - Renal failure
  - Turner syndrome
  - Down syndrome

CSF = cerebrospinal fluid.

[a] Modified with permission from Friedman DI, et al, Neurology.[34] © 2013 American Academy of Neurology.

Freidman, D Headaches due to low and high intracranial pressure
Continuum 2018;24(4) Headache:1066-1091

Imaging Abnormalities in Intracranial Hypertension

Presumed Mechanism	Findings	Pooled Sensitivity [95% CI]	Pooled Specificity [95% CI]
Bony erosion from IIH	Empty sella	80% [71–89] (11,12)	83% [76–90] (8–10)
	CSF leak	NA	NA
	Meningocele/meningoencephalocele	11% [4–18]* (39)	0% [NA]* (39)
	Foramen ovale widening	50% [36–64]* (20)	80% [69–91]* (20)
Mechanical deformation from IIH	Posterior flattening of the posterior poles	66% [60–72] (8–10,12,19,20)	98% [96–100] (8–10,20)
	Optic nerve head protrusion	36% [28–44] (8–10,12,19,20)	99% [98–100] (8–10,20)
	Distention of the optic nerve sheath	58% [48–68] (9,10,12)	89% [85–95] (9,10)
	Vertical tortuosity of the optic nerve	43% [37–50] (8–10,12,19,20)	90% [85–95] (8–10,20)
	Transverse sinus venous stenosis	97% [93–100] (55,64,66)	93% [84–97]* (55)
Papilledema	Enhancement of the optic nerve head	17% [11–23] (8–10,19)	99% [97–100] (8–10)
Uncertain	Tonsillar herniation ≥5 mm	16% [10–22] (9,34,37)	95% [91–100] (9,34)

Pooled sensitivity and specificity were obtained from at least 2 studies using the same criteria to define the findings.
*Obtained from one single study (provided by the authors or recalculated).

Bidot, Samuell, et al. Brain Imaging in Idiopathic Intracranial Hypertension .Journal of Neuro-Ophthalmology35(4):400-411, December 2015.

Papilledema

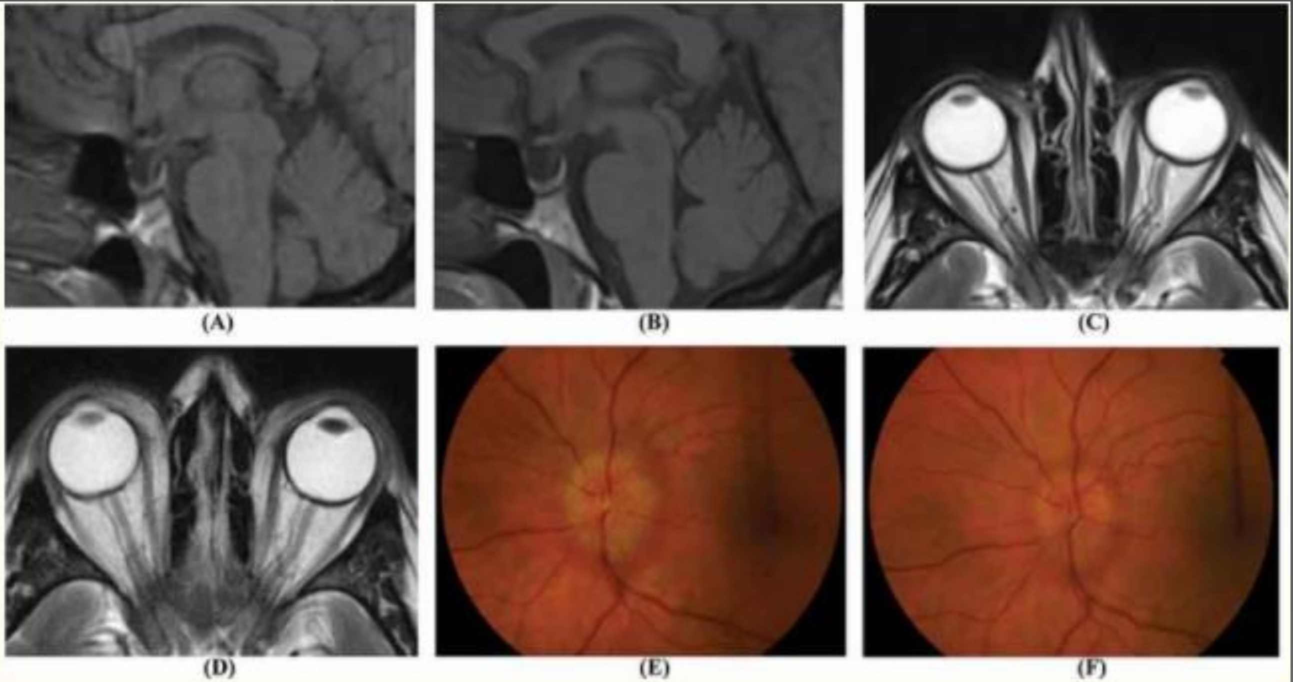

Magnetic resonance imaging, active versus resolved papilloedema. One patient from the resolved papilloedema group underwent MRI during active papilloedema and after resolution of papilloedema (images taken 2 years apart). MRI demonstrated empty sella both before (A) and after (B) resolution of papilloedema. MRI also demonstrated protrusion of the ONH into the globe both before (C) and after (D) resolution of papilloedema. Images of the patient's left optic disc also demonstrated grade III papilloedema (E) and grade 0 papilloedema (F) taken within 4 weeks of the above MRI images.

- Prevalence of papilledema in patients with IIH 94.3%

Chang, R. O., et al.(2016). Neuroimaging Features of Idiopathic Intracranial Hypertension Persist After Resolution of Papilloedema. *Neuro-ophthalmology (Aeolus Press)*, *40*(4), 165–170.
Digr e, K. B., et al.(2009). A comparison of idiopathic intracranial hypertension with and without papilledema. *Headache*, *49*(2), 185–193.

Empty Sella

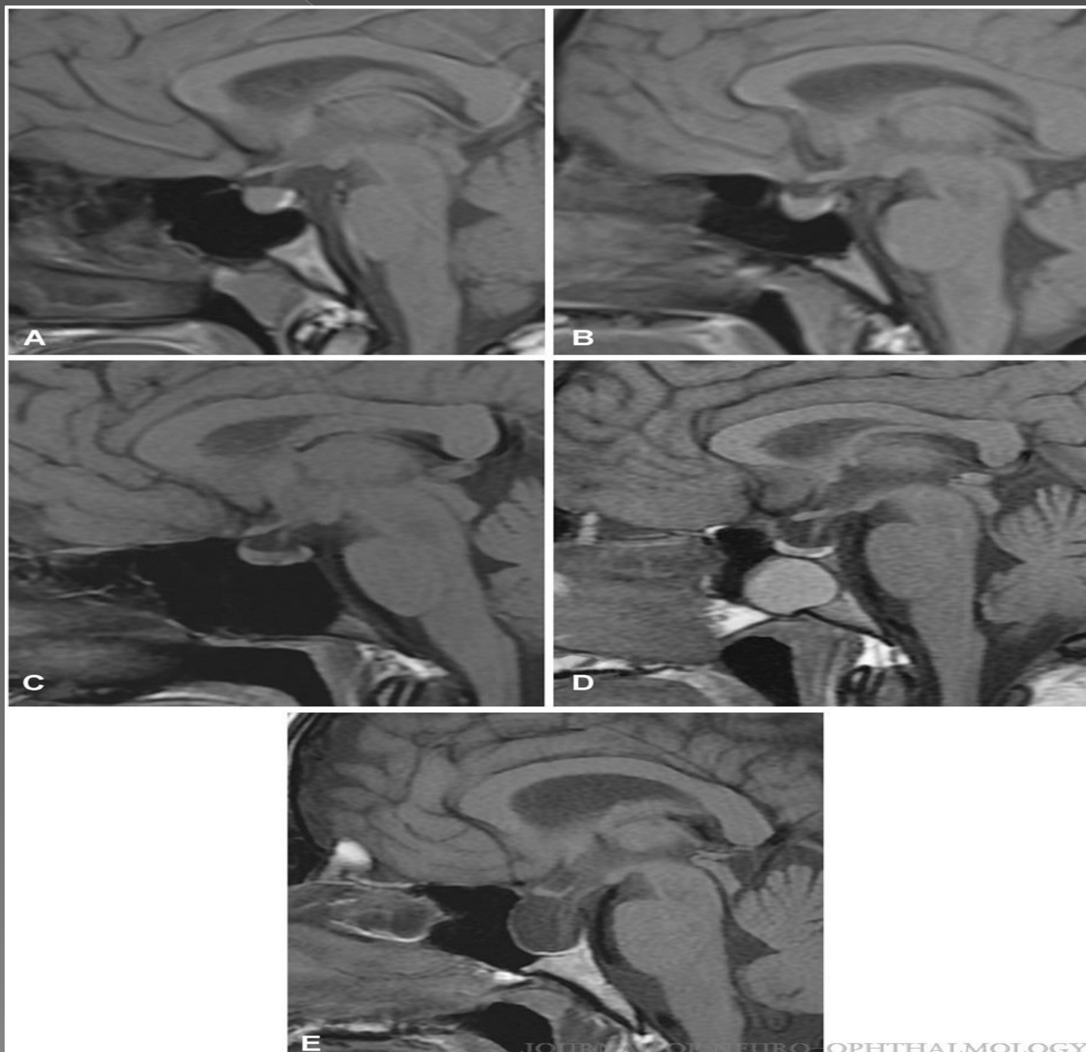

- Most frequently reported finding in imaging of IIH

FIG. 1

Precontrast mid-sagittal T1 magnetic resonance imaging (MRI) of empty sella based on the classification of Yuh et al ([11]). **A.** Category I, normal. The anterior aspect of the pituitary gland appears isointense with brain and fills the sella turcica. **B.** Category II, mild superior concavity, less than 1/3 height of the sella turcica. **C.** Category III, moderate concavity, between 1/3 and 2/3 height of the sella turcica. **D.** Category IV, severe concavity, more than 2/3 height of the sella turcica. **E.** Category V, no pituitary tissue visible. A partially empty sella is defined by Grade III and IV and an empty sella by Grade V.

Bidot, Samuell, et al. Brain Imaging in Idiopathic Intracranial Hypertension .Journal of Neuro-Ophthalmology35(4):400-411, December 2015

Posterior Globe Flattening and Optic Nerve Head Protrusion

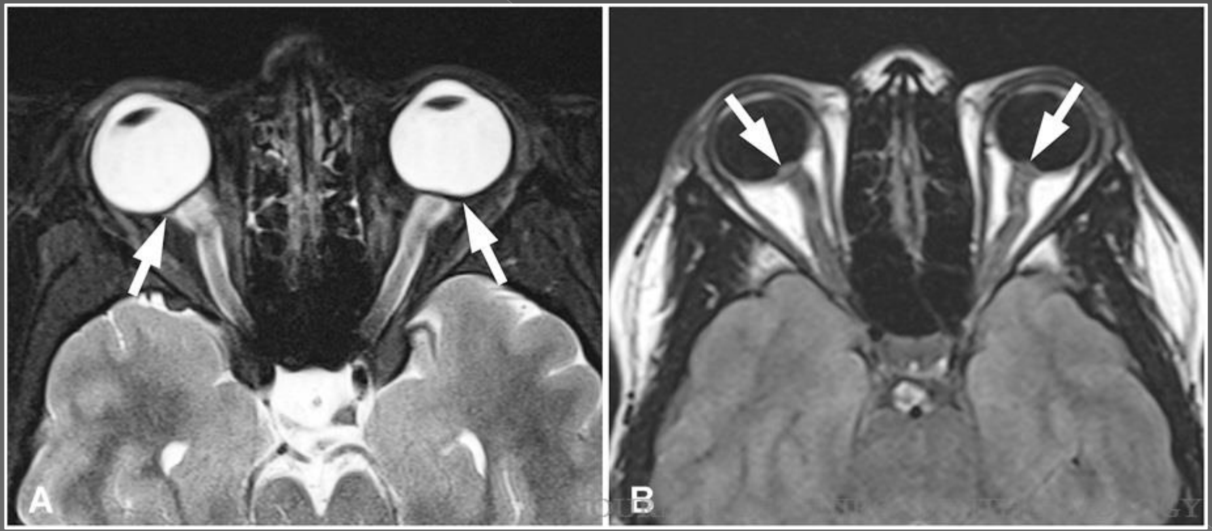

Bidot, Samuell, et al. Brain Imaging in Idiopathic Intracranial Hypertension .Journal of Neuro-Ophthalmology35(4):400-411, December 2015.

FIG. 2: A. Axial T2 fat-saturated scan shows flattening of the posterior globes (arrows) around the insertion of the optic nerve. **B.** There is protrusion of the optic nerve head into the vitreous cavity (arrows) on axial fluid-attenuated inversion recovery (FLAIR) image.

Optic Disc Enhancement and Distention of Optic Nerve Sheaths

Postcontrast axial T1 magnetic resonance imaging (MRI) with fat suppression reveals enhancement of the optic nerve head (arrow). Flattening of the posterior globes is seen bilaterally.

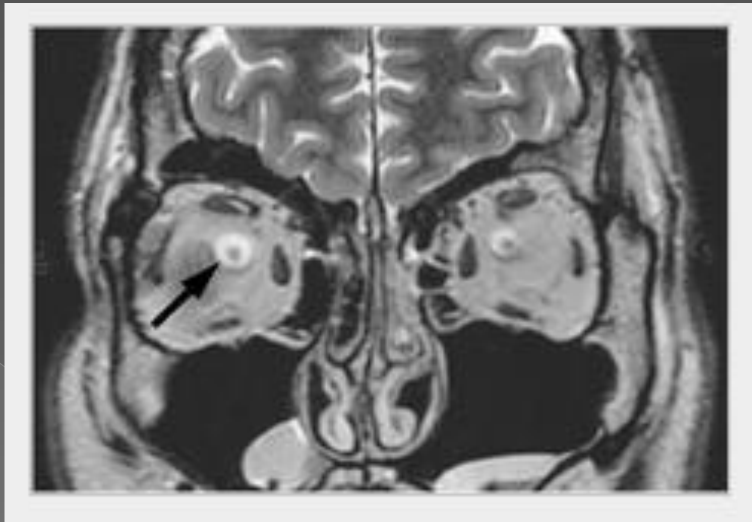

Coronal T2 orbital magnetic resonance imaging (MRI). Distention of the optic nerve sheath (described as "optic nerve unfoldment" anatomically (27)) appears as an enlarged cerebrospinal fluid (CSF) ring surrounding the optic nerve (arrow).

Bidot, Samuell, et al. Brain Imaging in Idiopathic Intracranial Hypertension .Journal of Neuro-Ophthalmology35(4):400-411, December 2015.

Vertical Tortuosity of the Optic Nerve

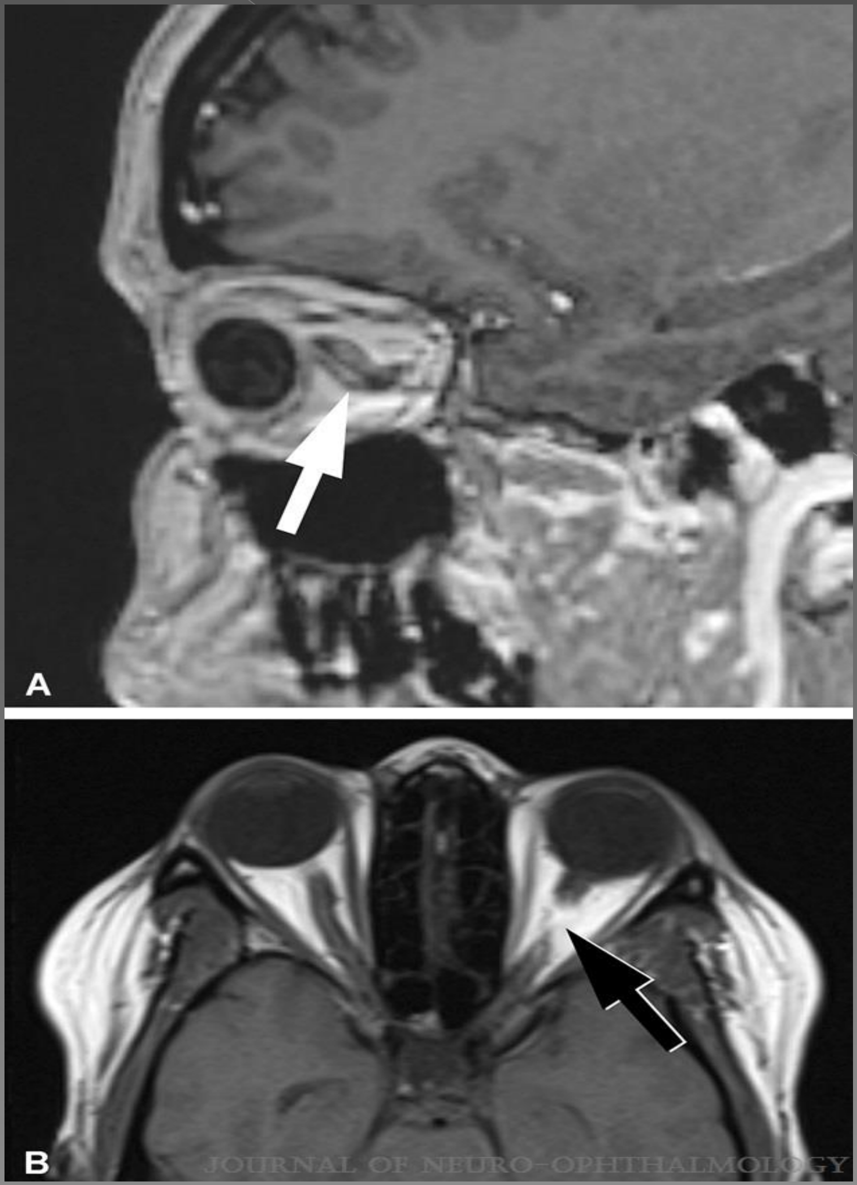

A. Postcontrast T1 magnetic resonance imaging (MRI) reformatted in a sagittal oblique plane shows vertical tortuosity of the right optic nerve following the shape of the letter "S" in its vertical component (arrow). B. Noncontrast axial T1 scan reveals that the left optic nerve cannot be entirely displayed along a single plane because the signal of orbital fat obscures the mid-portion of the nerve (arrow) ["smear sign" (8)].

Bidot, Samuell, et al. Brain Imaging in Idiopathic Intracranial Hypertension .Journal of Neuro-Ophthalmology35(4):400-411, December 2015.

Cerebellar Tonsillar Herniation

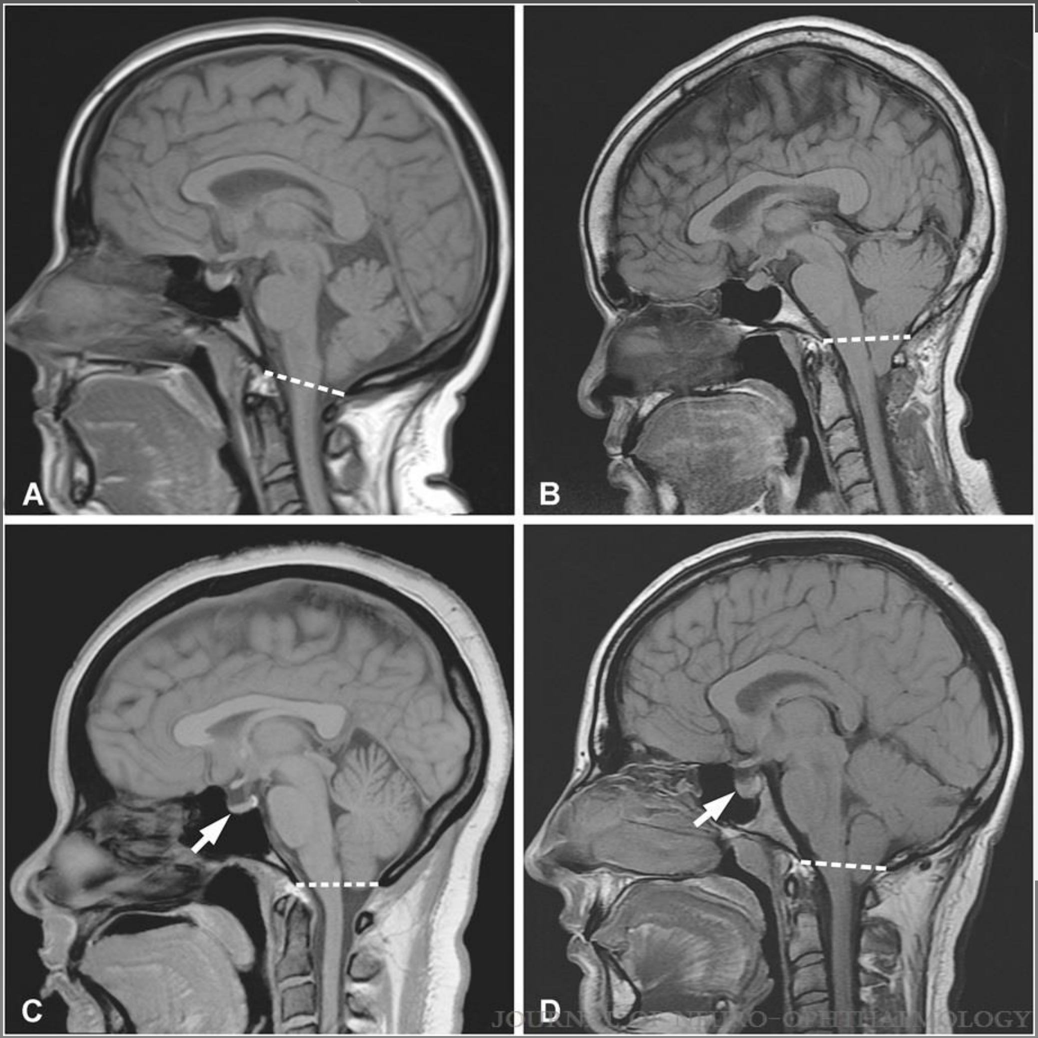

FIG. 6: Noncontrast T1 mid-sagittal magnetic resonance imaging (MRI) with dashed line (McRae line) from the basion to the opisthion, defining the foramen magnum.**A**. Normal position of the cerebellar tonsils with respect to the foramen magnum in an IIH patient. The inferior pole of the cerebellar tonsils normally lies at the level of or just above the foramen magnum. **B**. Chiari I malformation (CM1). CM1 is generally believed to be congenital and diagnosed on strict radiologic criteria, including downward extension of peg-shaped cerebellar tonsils at least 5 mm below the foramen magnum without mass or other cause of acquired tonsillar herniation. For borderline cases (tonsillar herniation ≥3 mm but <5 mm), the association with other radiologic findings commonly seen in CM1, such as syringomyelia or kinking of the cervico-medullary junction, help establish the diagnosis. **C**. Cerebellar tonsillar ectopia refers to the low-lying configuration of the tonsils, up to 2 or 3 mm below the foramen magnum. A partially empty sella (Category IV) is also present (arrow). **D**. CM1-like configuration of the cerebellar tonsils in a patient with IIH. Cerebellar tonsils extend to 10 mm below the foramen magnum. In addition, there is a partially empty sella, (Category III) (arrow).

Bidot, Samuell, et al. Brain Imaging in Idiopathic Intracranial Hypertension .Journal of Neuro-Ophthalmology35(4):400-411, December 2015

Meningoceles

A. Coronal thin section computed tomography (CT) demonstrates a bony defect (arrow) in the skull base. Meningocele/meningoencephalocele and sequestered secretions in the sphenoid sinus have the same appearance. B. Coronal T2 magnetic resonance image of same patient as in A shows that sphenoid sinus abnormality is composed of brain tissue. C. Axial T2 scan reveals meningoceles involving both of Meckel caves (arrows).

Bidot, Samuell, et al. Brain Imaging in Idiopathic Intracranial Hypertension .Journal of Neuro-Ophthalmology35(4):400-411, December 2015.

Imaging in Pediatrics

- Study comparing images of 16 adults and 23 children with IIH found no significant differences
- Empty sella less prevalent in pediatric populations
  - 26% pediatric vs. 69% adults

Bidot, Samuell, et al. Brain Imaging in Idiopathic Intracranial Hypertension .Journal of Neuro-Ophthalmology35(4):400-411, December 2015.

Intracranial Venous Sinus Stenting: A Review of Idiopathic Intracranial Hypertension and Expanding Indications

Monitoring Editor: Alexander Muacevic and John R Adler

Lekhaj C Daggubati[1] and Kenneth C Liu[2]

Idiopathic intracranial hypertension (IIH) is a functionally limiting disorder secondary to increased intracranial pressures (ICPs) with a prevalence of one per 100,000 persons. It is estimated to cost >$400 million per year in productively. Symptoms classically consist of chronic headaches, papilledema, and visual loss. The pathophysiology is unknown but postulated to involve increased resistance to cerebrospinal fluid (CSF) absorption. Traditional treatments involve weight loss, acetazolamide, CSF diversion, or optic nerve fenestration. More recent technology has allowed exploration of venous sinus stenosis. Through venous sinus stenting (VSS), the ICPs and venous sinus pressures decrease. After treatment, >75% exhibit an improvement in headaches, ~50% improvement in tinnitus, and ~50 % improvement in ophthalmologic testing. Complications are rare but involve stent stenosis, femoral pseudoaneurysm, and h

expansion to other veno

Figure 1. Patient number 4. (a) Pre-stenting venographic injection showing a 70% transverse sinus stenosis (arrow) (b), (c) immediate post-stent placement venographic injection and CT venography showing wide patency of the stented venous sinus and contrast filling (arrows).

Koovor JM, et al. Transverse venous sinus stenting for idiopathic intracranial hypertension: Safety and feasibility. Neuroradiol J. 2018 Oct;31(5):513-517.

Intracranial Venous Sinus Stenting: A Review of Idiopathic Intracranial Hypertension and Expanding Indications

Monitoring Editor: Alexander Muacevic and John R Adler

Lekhaj C Daggubati[1] and Kenneth C Liu[2]

Treatments for IIH

- Medication
- Serial lumbar punctures
- Optic nerve sheath fenestration
- Ventriculoperitoneal shunt
- Lumboperitoneal shunt
- Venous sinus stenting (1995)
- Lifestyle Changes
  - Weight loss shown to improve papilledema

Pressure Headaches

- Spontaneous Intracranial Hypotension is underdiagnosed and should be considered in refractory headaches patients.
- The imaging of for SIH is not always easy and may not always identify the leak. There are several strategies and areas to look
- Thorough ophthalmology evaluation is critical to identifying patients with IIH
- Imaging has shown to be helpful in further identifying IIH in patients using MRI and MRV

Questions ???
Thank you
(special thanks to Megan Rooney for her assistance)